

# Microstructure in polypropylenes prepared with $\text{TiCl}_4/\text{MgCl}_2\text{-Et}_3\text{Al}$ and $\text{Ti}(\text{OBu})\text{Cl}_3/\text{MgCl}_2\text{-Et}_3\text{Al}$ catalytic systems

Tetsuo Hayashi, Yoshio Inoue\* and Riichirô Chûjô

Department of Polymer Chemistry, Tokyo Institute of Technology, 12-1, O-okayama 2-chome, Meguro-ku, Tokyo 152, Japan

and Yoshiharu Doi

Research Laboratory of Resource Utilization, Tokyo Institute of Technology, 4529 Nagatsuda-cho, Midori-ku, Yokohama 227, Japan

(Received 13 October 1988; revised 9 January 1989; accepted 17 January 1989)

Microstructures were studied for polypropylenes prepared with  $\text{TiCl}_4/\text{MgCl}_2\text{-Et}_3\text{Al}$  and  $\text{Ti}(\text{OBu})\text{Cl}_3/\text{MgCl}_2\text{-Et}_3\text{Al}$  catalytic systems. Pentad tacticities, chain-end structures, and regioirregularity in these polypropylenes were determined from  $^{13}\text{C}$  n.m.r.,  $^1\text{H}$  n.m.r., and INEPT (insensitive nuclei enhancement by polarization transfer) spectra. The propylene polymerization mechanism was statistically analysed on the basis of the two-site model from the pentad tacticities. It was confirmed that these polypropylenes are composed of the isotactic and atactic polymers produced at the IPP and APP catalytic sites, which produce the isotactic and atactic polymers, respectively. The optimum values of the two-site model parameters elucidated that the displacement of Cl ligand around the titanium by OBU reduces the strength of the steric control at the IPP site. The detected chain-end structures verified that the chain transfer of propagation species to the propylene monomer terminates the propagation reaction and regenerates initiation species. The two-site model analysis for the tactic structures at the chain-end indicated that the steric controls of the initiation reactions at both sites are as strong as those of propagation reactions. Further, it was found that these polypropylenes contain head-to-head and tail-to-tail structures whose contents (monomer unit per chain) are  $10^{-3}$  order.

(Keywords: polypropylene; Ziegler-Natta catalyst;  $^{13}\text{C}$  n.m.r.;  $^1\text{H}$  n.m.r.; tacticity; chain-end structure; polymerization mechanism; propylene polymerization)

## INTRODUCTION

Since the discovery of Ziegler-Natta catalysts, a number of workers have investigated a large number of different combinations of metal alkyls and transition metal salts to make catalytic systems which are active for polymerization of ethylene, propylene and higher olefins, and copolymerization of these monomers. In recent years, supported catalysts have been used for the industrial scale process of ethylene<sup>1-6</sup> and propylene polymerization<sup>7-9</sup>, because these catalysts were shown to be highly efficient.

$^{13}\text{C}$  n.m.r. is the most powerful method to determine the microstructures in polypropylene. Tactic and chain-end structures, and the regioirregularity in polypropylenes have been investigated in detail from the high resolution  $^{13}\text{C}$  n.m.r. spectra.  $^{13}\text{C}$  n.m.r. assignments of methyl carbons in pentad and heptad stereoisomers have been confirmed by the chemical shift calculation using the gamma-effect on  $^{13}\text{C}$  n.m.r. chemical shift and rotational isomeric state model<sup>10,11</sup>. A mechanism of stereospecific polymerization has been statistically analysed from the values of tacticities in polypropylenes prepared with various Ziegler-Natta catalytic systems<sup>10-16</sup>. The two-site model<sup>13,14</sup>, in which at one site propylene polymerization proceeds according to the asymmetric Bernoullian statistics (selection

between dextro and levo<sup>17</sup>) and at the other site to symmetric Bernoullian statistics (selection between meso and racemo), has been found to be adequate for the description of the propylene polymerization mechanism<sup>11,15,16</sup>.

Analyses of chain-end structures in polypropylene have thrown light on the study of the mechanisms of the initiation and termination reactions. Zambelli *et al.*<sup>18-21</sup> elucidated the mechanism of the initiation and termination reactions of propylene polymerization with various types of Ziegler-Natta catalytic systems from the  $^{13}\text{C}$  n.m.r. spectra of  $^{13}\text{C}$  enriched polypropylenes and selectively  $^{13}\text{C}$  enriched end groups of polypropylenes. In an earlier paper<sup>22</sup>, we determined the chain-end structures in polypropylene prepared with  $\delta\text{-TiCl}_3/\text{Et}_2\text{AlCl}$  catalytic system in the presence of hydrogen. Triad and tetrad tacticities at the chain-end have been evaluated from the quantitative analyses of the split peaks arising from the different tactic structures at the chain-end<sup>22</sup>. These results have provided useful information on steric controls of the initiation reaction.

Regioirregularity in polypropylene chains has been studied from the  $^{13}\text{C}$  n.m.r. spectra<sup>23-25</sup>. Asakura *et al.*<sup>25</sup> calculated the  $^{13}\text{C}$  chemical shifts due to the gamma-effect of carbons in regioirregular polypropylene by taking into account the effect of tacticity on chemical shifts. Their calculated shifts are in good agreement with the observed

\* To whom correspondence should be addressed

ones, and with the calculated ones<sup>23</sup> based on the empirical rule.

The analysis of microstructures in polypropylene prepared with supported catalysts is of great interest, because microstructures in polypropylenes reflect the kinetic schemes and steric control of the propylene polymerization as mentioned above. In this study, the microstructures in polypropylenes prepared with supported catalytic systems,  $\text{TiCl}_4/\text{MgCl}_2\text{-Et}_3\text{Al}$  and  $\text{Ti}(\text{OBu})\text{Cl}_3/\text{MgCl}_2\text{-Et}_3\text{Al}$ , in the absence of hydrogen are studied by  $^{13}\text{C}$  and  $^1\text{H}$  n.m.r. spectroscopy, and the polymerization mechanism is statistically analysed on the basis of the two-site model from the pentad tacticities. The chain-end structures are also determined by  $^{13}\text{C}$  and  $^1\text{H}$  n.m.r. spectra. Proton decoupled INEPT (insensitive nuclei enhanced by polarization transfer)<sup>26,27</sup> spectra obtained with the delay times ( $\Delta$ ) of  $3/4J$  and  $2/4J$  prior to the data acquisition are used for the spectral assignments of carbons situated at the chain-end and at the inverted propylene units. The initiation and termination reactions of propylene polymerization are elucidated from the chain-end structures.

## EXPERIMENTAL

### Polypropylenes

Polypropylenes A and B were prepared with  $\text{TiCl}_4/\text{MgCl}_2\text{-Et}_3\text{Al}$  and  $\text{Ti}(\text{OBu})\text{Cl}_3/\text{MgCl}_2\text{-Et}_3\text{Al}$  catalytic systems, respectively. Polymerization was performed at  $40^\circ\text{C}$  for 2 h under atmospheric pressure (pressure of propylene = 660 T). n-Heptane was used as the polymerization medium. Samples AS6 and BS6 are fractions of A and B soluble in boiling hexane, respectively. Weight fractions of AS6 and BS6 to the whole polymers A and B are 0.53 and 0.63, respectively. The weight average ( $\bar{M}_w$ ) and number average ( $\bar{M}_n$ ) molecular weights of polypropylenes were determined by g.p.c.. A molecular weight calibration curve for polypropylene was obtained on the basis of the universal calibration<sup>28,29</sup> curve for polystyrene determined from seven standard polystyrenes of molecular weights from 950 to 6 750 000. In Table 1 are shown the molecular weights of these samples. The values of molecular weights for AS6 and BS6 have ambiguity due to the poor reliability of the calibration curve in the range of molecular weight less than 1000 (the lowest molecular weight of standard polystyrenes is 950), because AS6 and BS6 have considerable amounts of low molecular weight components less than 1000. AS6 and BS6 were used for the analysis of chain-end structures.

### N.m.r. measurement

$^{13}\text{C}$  and  $^1\text{H}$  n.m.r. spectra were recorded at  $120^\circ\text{C}$  on a Jeol GSX-270 FT spectrometer operated at 67.8 and 270.1 MHz, respectively. The sample solutions in 10 mm o.d. glass tube were prepared in *o*-dichlorobenzene (90 vol%)/benzene- $d_6$  (10 vol%) to give 0.15 g (polymer)

**Table 1** Molecular weights of polypropylene samples

Sample	$\bar{M}_w$	$\bar{M}_n$	$\bar{M}_w/\bar{M}_n$
A	190 000	14 000	13.6
AS6	ca. 50 000	ca. 8 000	ca. 6.3
B	140 000	14 000	10.0
BS6	ca. 50 000	ca. 8 000	ca. 6.3

$\text{cm}^{-3}$  (solvent). Benzene- $d_6$  was used for the  $^2\text{H}$  n.m.r. internal lock.

In  $^{13}\text{C}$  n.m.r. measurements, broad band noise decoupling was used to remove  $^{13}\text{C}\text{-}^1\text{H}$  couplings. The pulse angle was  $90^\circ$ , and 8000 free induction decays were stored in 64K data points using a spectral window of 12 000 Hz. For the quantitative measurement, the pulse repetition time was set to be 25 s, which is more than five times the spin-lattice relaxation times of the most mobile methyl carbons at the chain-end (4.0–4.8 s (ref. 30)).

The  $^1\text{H}$  decoupled INEPT method<sup>26,27</sup>, in which the delay times ( $\Delta$ ) prior to data acquisition are  $3/4J$  and  $2/4J$  (where  $J$  is a  $^1\text{H}\text{-}^{13}\text{C}$  spin-spin coupling constant), was used to discriminate methylene peaks from methine peaks and the selective observation of methine peaks, respectively.

In  $^1\text{H}$  n.m.r. measurement, the pulse angle was  $90^\circ$ , and 500 free induction decays were stored in 32K data points using a spectral window of 10 000 Hz.

In all measurements hexamethyldisiloxane was used as an internal reference (2.03 ( $^{13}\text{C}$ ) and 0.07 ( $^1\text{H}$ ) ppm downfield from the resonances of tetramethylsilane).

## RESULTS AND DISCUSSION

### Tactic structures

In Figures 1a and b are shown the methyl resonance regions of  $^{13}\text{C}$  n.m.r. spectra of samples A and B, and AS6 and BS6, respectively. The  $^{13}\text{C}$  n.m.r. chemical shift assignments of methyl pentad peaks proposed by Zambelli *et al.*<sup>31</sup>, which have been confirmed from the chemical shift calculation via the gamma effect<sup>10,11</sup> are also shown in Figure 1b. Pentad tacticities were accurately determined from the relative peak areas using curve resolution method<sup>12</sup> as listed in Table 2. From these data propylene polymerization mechanism was analysed on the basis of the two-site model<sup>11,13–16</sup>. The parameters of this model and their meanings are as follows:

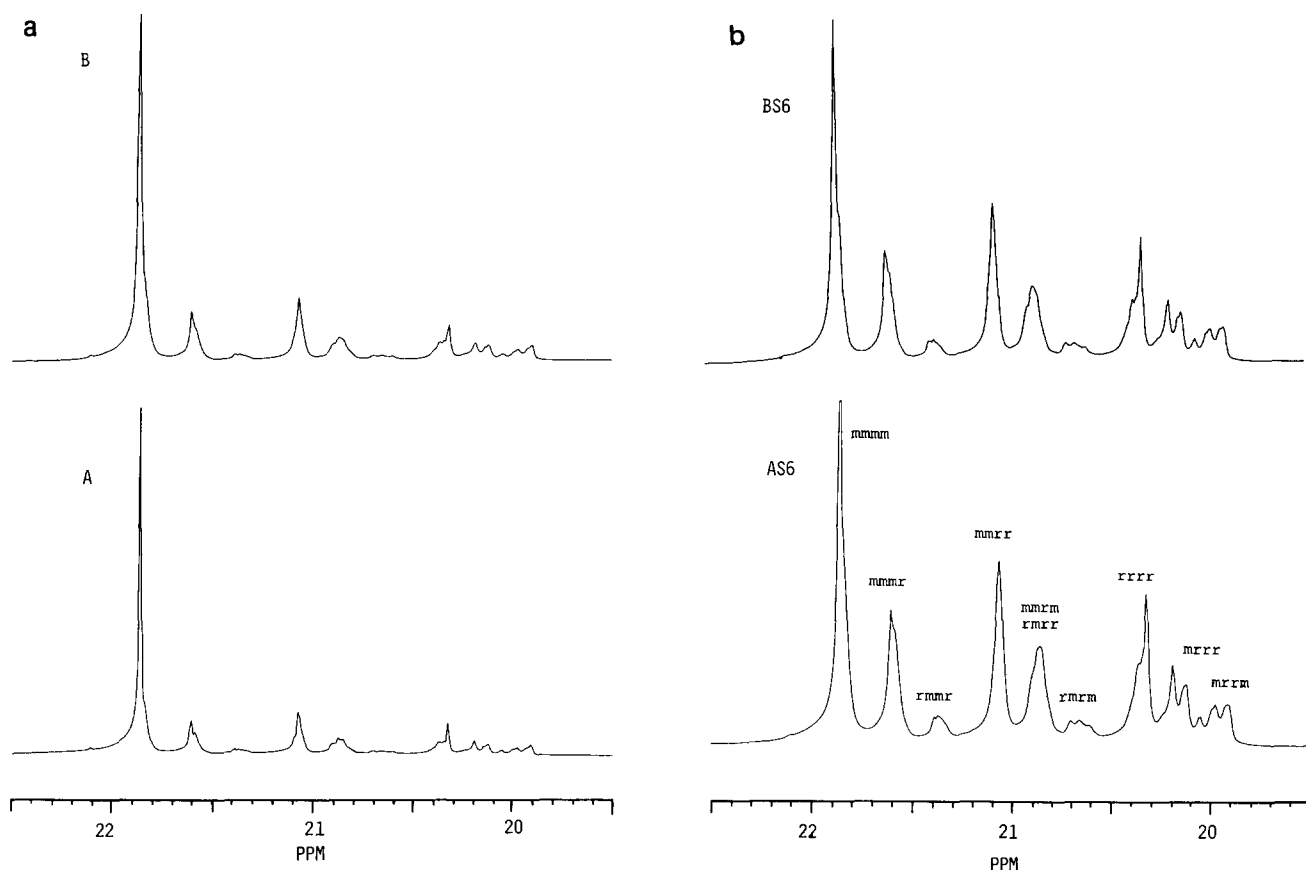
$\alpha$ , the probability of selecting a d(dextro)-unit at a d-preferring site in the asymmetric Bernoullian model site;

$\sigma$ , the probability of selecting a meso dyad configuration in the symmetric Bernoullian model site;

$\omega$ , the weight fraction of the polymer produced at the asymmetric Bernoullian model site.

The optimum values of model parameters were determined by the nonlinear least squares method. The results are shown in Table 3. Pentad stereosequence distributions in samples A, B, AS6, and BS6 predicted by the two-site model are in good agreement with those determined experimentally within standard deviations of less than  $5.0 \times 10^{-3}$ , indicating the suitability of the two-site model for the mechanism of propylene polymerization. Optimum values of these parameters indicate that the isotactic polymer is predominantly produced at the asymmetric model site (IPP-site) and the atactic polymer at the symmetric model site (APP-site). This conclusion is in agreement with our previous study<sup>11,14–16</sup>.

As shown in Figure 1a (Sample A (top), Sample B (bottom)) and Table 2, fractions of mmmr, mmrr, and mrrm in B are larger than those in A. This result is


**Figure 1** Methyl resonance regions in  $^{13}\text{C}$  n.m.r. spectra of (a) polypropylenes A and B and (b) AS6 and BS6

**Table 2** Pentad tacticities of polypropylenes

Sample pentad	A		B		AS6		BS6	
	observed	calculated <sup>a</sup>	observed	calculated <sup>a</sup>	observed	calculated <sup>a</sup>	observed	calculated <sup>a</sup>
mmmm	0.646	0.647	0.605	0.607	0.265	0.264	0.294	0.297
mmmr	0.052	0.053	0.075	0.075	0.111	0.114	0.111	0.111
rmmr	0.014	0.010	0.013	0.010	0.030	0.026	0.027	0.022
mmrr	0.061	0.064	0.082	0.085	0.141	0.131	0.123	0.126
mrrm	0.059	0.059	0.060	0.057	0.130	0.134	0.119	0.121
rmrr								
rmrm	0.020	0.020	0.020	0.021	0.048	0.052	0.050	0.044
mrrm	0.037	0.032	0.045	0.042	0.070	0.066	0.060	0.064
mrrr	0.048	0.050	0.043	0.047	0.092	0.099	0.092	0.093
rrrr	0.063	0.065	0.057	0.056	0.113	0.114	0.124	0.122
$\text{SD}^b/10^{-3}$		2.73		2.54		4.99		3.40

<sup>a</sup> Based on the two-site model. Parameters for the calculation are listed in Table 3

<sup>b</sup> Standard deviations between the observed and calculated fractions of pentad stereoisomers

**Table 3** The optimum values of the parameters for the two-site model

Sample	$\omega$	$\alpha$	$\sigma$
A	0.770	0.966	0.273
B	0.797	0.947	0.281
AS6	0.640	0.836	0.270
BS6	0.660	0.851	0.243

reasonably described by using optimum values of model parameters as follows.

The mmmr, mmrr, and mrrm sequences are isolated rr defects in the isotactic polypropylene chains and the peak assigned to mmmr pentad arises mainly from

mmmmrr heptad<sup>11</sup>. The optimum value (0.966) of  $\alpha$  for sample A (prepared with  $\text{TiCl}_4/\text{MgCl}_2$  catalyst) is larger than that (0.947) for sample B (prepared with  $\text{Ti}(\text{O}i\text{Bu})\text{Cl}_3/\text{MgCl}_2$  catalyst), although the difference is small. This elucidates that the displacement of Cl ligand around the titanium by *O*Bu reduces the strength of the steric control at the IPP site.

As shown in Figure 1b and Table 2, the pentad tacticities of boiling hexane soluble fractions AS6 and BS6 are close to each other. The values of parameter  $\alpha$  for AS6 and BS6 are different from those of whole polymers, A and B (Table 3), while the values of  $\sigma$  are almost constant among these polymers. This indicates



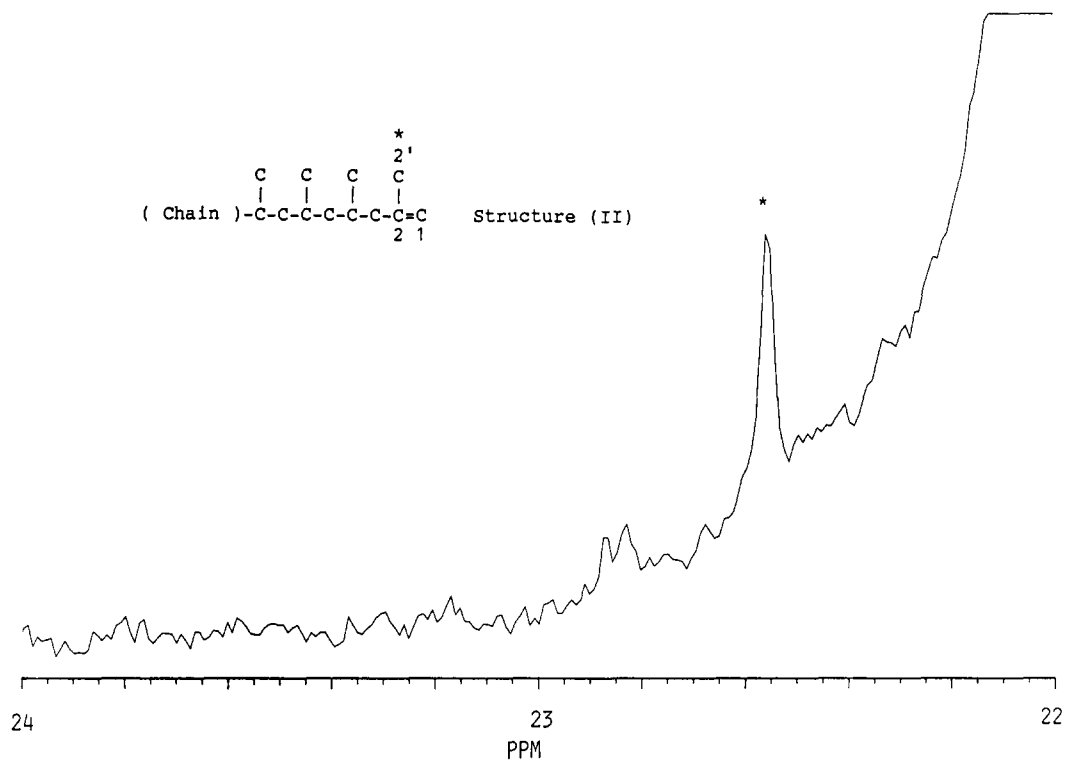


Figure 4 The region from 22 to 24 ppm in  $^{13}\text{C}$  n.m.r. spectrum of AS6

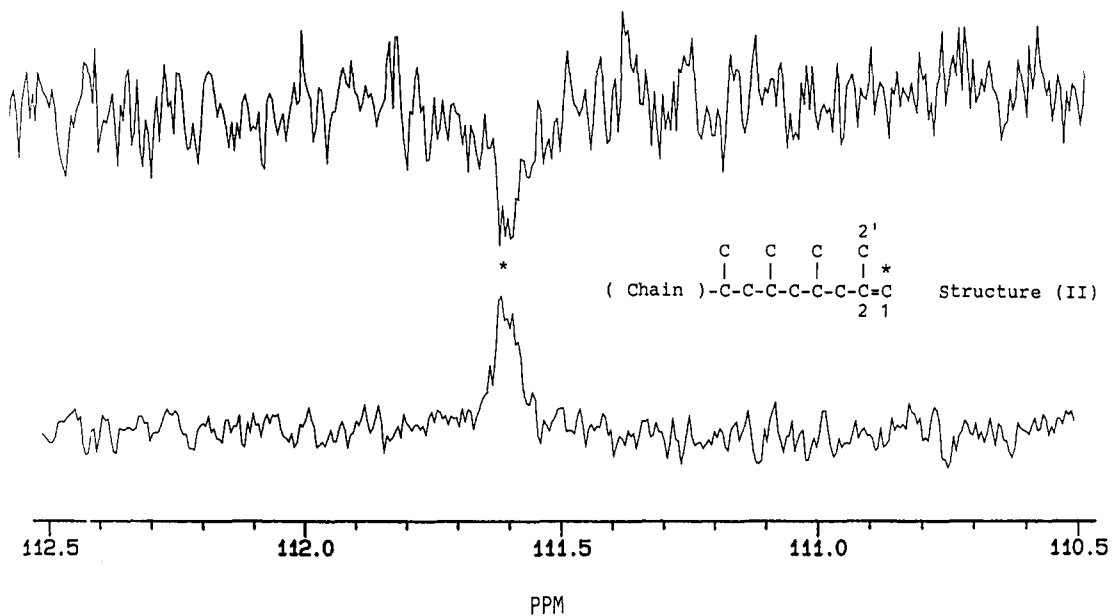


Figure 5 Regions from 110.5 to 112.5 ppm in  $^{13}\text{C}$  n.m.r. (bottom) and INEPT ( $\Delta = 3/4J$ ) spectra of AS6.  $^1\text{H}$ - $^{13}\text{C}$  spin-spin coupling constant,  $J$ , is set to be 160 Hz

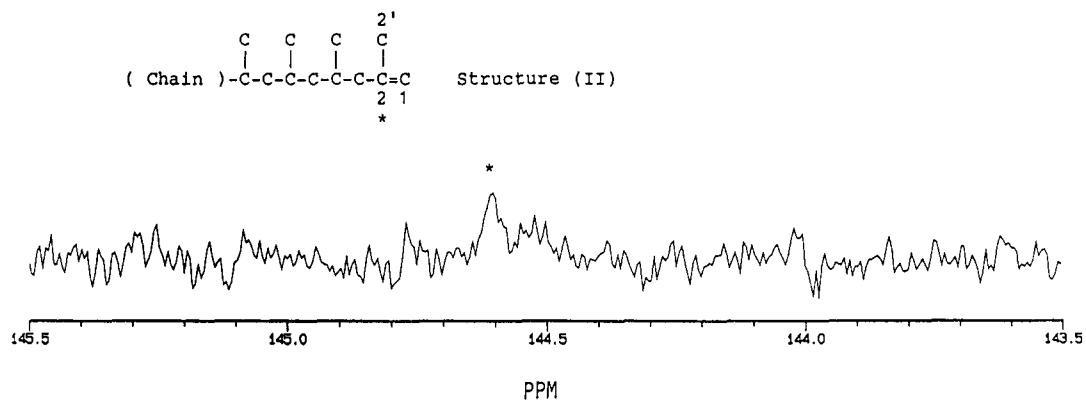


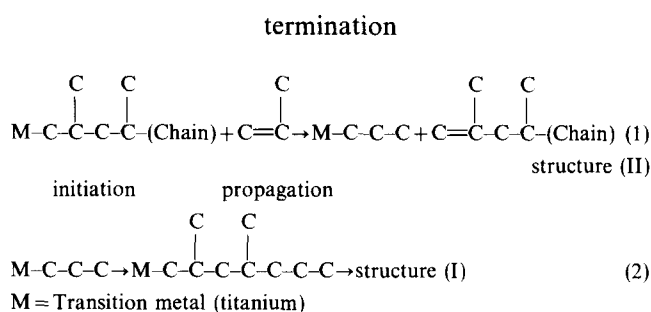
Figure 6 The region from 143.5 to 145.5 ppm in  $^{13}\text{C}$  n.m.r. spectrum of AS6

In Figure 6, a small peak observed at 144.6 ppm is assigned to carbon 2 in structure (II). The reason for the small intensity of this peak is attributable to the long spin-lattice relaxation time and the ineffective NOE of carbon 2, because this carbon being at the chain-end may be highly mobile, and further it has no directly attached protons.

In Figure 7 is shown the  $^1\text{H}$  n.m.r. spectrum of sample AS6. Two peaks observed at 4.67 and 4.73 ppm are assigned to the protons attached to methylene carbon 1 in structure II, referring to the  $^1\text{H}$  n.m.r. spectrum of 2,4-dimethyl-1-pentene<sup>34</sup>.

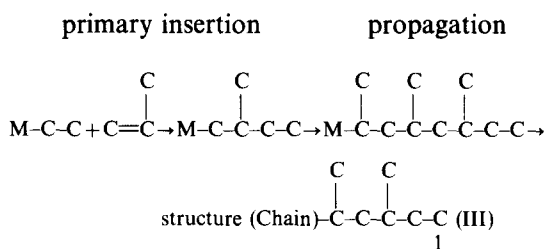
#### Schemes for the formation of chain-end structures

Under the polymerization conditions employed in this study, the termination and initiation reactions are expected to occur through the chain transfer reaction of the propagating species to the propylene monomer. In the case of the primary insertion of propylene, chain-end structures I and II are formed as follows.



According to the well known schemes for the initiation reaction<sup>35</sup>, the initiating species produced at the initial stage of the polymerization should be M-Et (where ethyl(Et) group is derived from  $\text{Et}_3\text{Al}$ ). The primary insertion to this species should produce chain-end

structure (III) as follows.



However, the peak of carbon 1 in structure III was not detected at about 11 ppm (ref. 22) in the spectrum of AS6. Thus, the relative content of this structure may be too small to be detected in the spectrum of the AS6 owing to the higher molecular weight ( $\bar{M}_n = 8000$ ) of boiling hexane soluble fraction (AS6), compared with that ( $\bar{M}_n = 1000$ ) of boiling heptane soluble fraction of polypropylene prepared with  $\delta\text{-TiCl}_3/\text{Et}_2\text{AlCl}$  catalytic system<sup>22</sup>. The number average molecular weight estimated from the relative areas of peaks of methyl carbon 1 in chain-end structure I and of inner-chain methyl carbon is 9300. Since the peak area of methyl carbon 1 in structure I is nearly equal to that of methyl carbon 2' in structure II, the value of  $M_n$  is reliable, indicating that most parts of polymer chains are formed by the chain transfer reaction.

Tacticity at the region of chain-end structure I is determined from the relative areas of split peaks of carbon 3, on the basis of the chain-end tetrad assignments<sup>22</sup> shown in Figure 3. The notations, PR-*mmm* (1), PR-*mmr* (2), . . . , and PR-*rrr* (8) denote a *n*-propyl group at the chain-end followed by dyad configurations of meso, meso, and meso(1), meso, meso and racemo(2), . . . , and racemo, racemo, and racemo(8) in the order from the chain-end. In Table 4 are shown the assignments of split peaks arising from PR-tetrad sequences. The triad

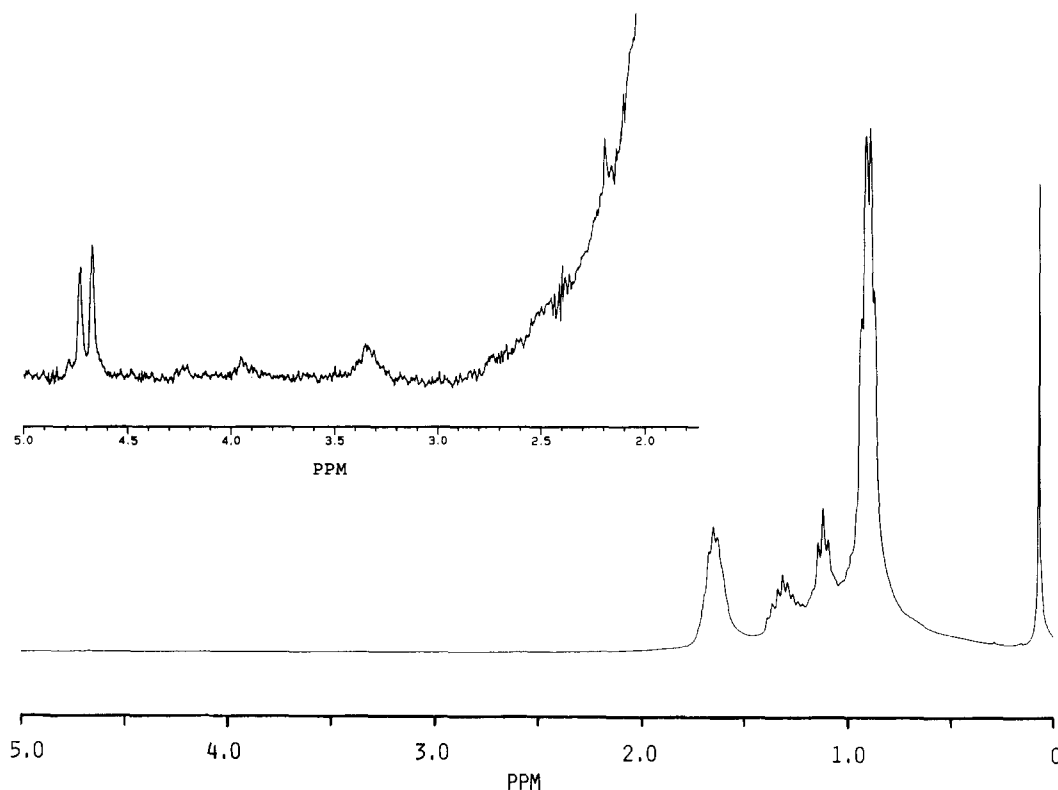
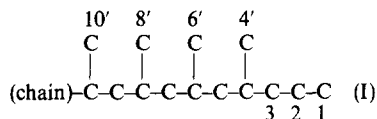


Figure 7  $^1\text{H}$  n.m.r. spectrum (bottom) of AS6 and the expanded spectrum (top) of the bottom

tacticity of chain-end structure I is similar to that of inner-chain as shown in Table 5. Further, fractions of PR-triads were well reproduced by the calculation using parameters of the two-site model. Optimum values of model parameters,  $\omega$ ,  $\alpha$ , and  $\sigma$  are 0.750, 0.785, and 0.289,

**Table 4** Chain-end tetrad assignments and individual fractions of split peaks of carbon 3 in structure (I) for AS6 (PR-tetrad is defined by the steric relationships among methyl carbons 4', 6', 8' and 10')



Chemical shift	Assignment PR-tetrad
39.81	PR- <i>mmm</i>
39.87	PR- <i>mrr</i>
40.04	PR- <i>mrr</i>
40.08	PR- <i>rrm</i>
40.68	PR- <i>rrm</i>
40.70	PR- <i>rrr</i>
40.84	PR- <i>rrr</i>
40.90	PR- <i>rmm</i>

respectively. These values are similar to those determined by the triad fractions of the inner chain. Thus, the steric controls of the initiation reactions at both sites are as strong as those of the propagation reactions, as confirmed for the polypropylene prepared with  $\delta$ -TiCl<sub>3</sub>/Et<sub>2</sub>AlCl catalytic system<sup>22</sup>.

#### Regioirregularity

In Figure 8 are shown the resonance regions from 31.0 to 39.0 ppm in <sup>13</sup>C n.m.r. and INEPT ( $\Delta = 2/4J$ ,  $3/4J$ ) spectra of AS6. From the INEPT ( $3/4J$ ) spectrum obtained with  $\Delta = 3/4J$ , it is found that peaks h, i, and j

**Table 5** The fractions of chain-end PR-triads and inner-chain triads for AS6

PR-triad	fraction		inner-chain triad	fraction observed
	observed	calculated <sup>a</sup>		
PR- <i>mm</i>	0.389	0.389	<i>mm</i>	0.406
PR- <i>mr</i>	0.164	0.178	<i>mr</i>	0.319
PR- <i>rm</i>	0.193	0.178		
PR- <i>rr</i>	0.254	0.254	<i>rr</i>	0.275

<sup>a</sup> Based on the two site model:  $\omega = 0.750$ ,  $\alpha = 0.785$ ,  $\sigma = 0.289$

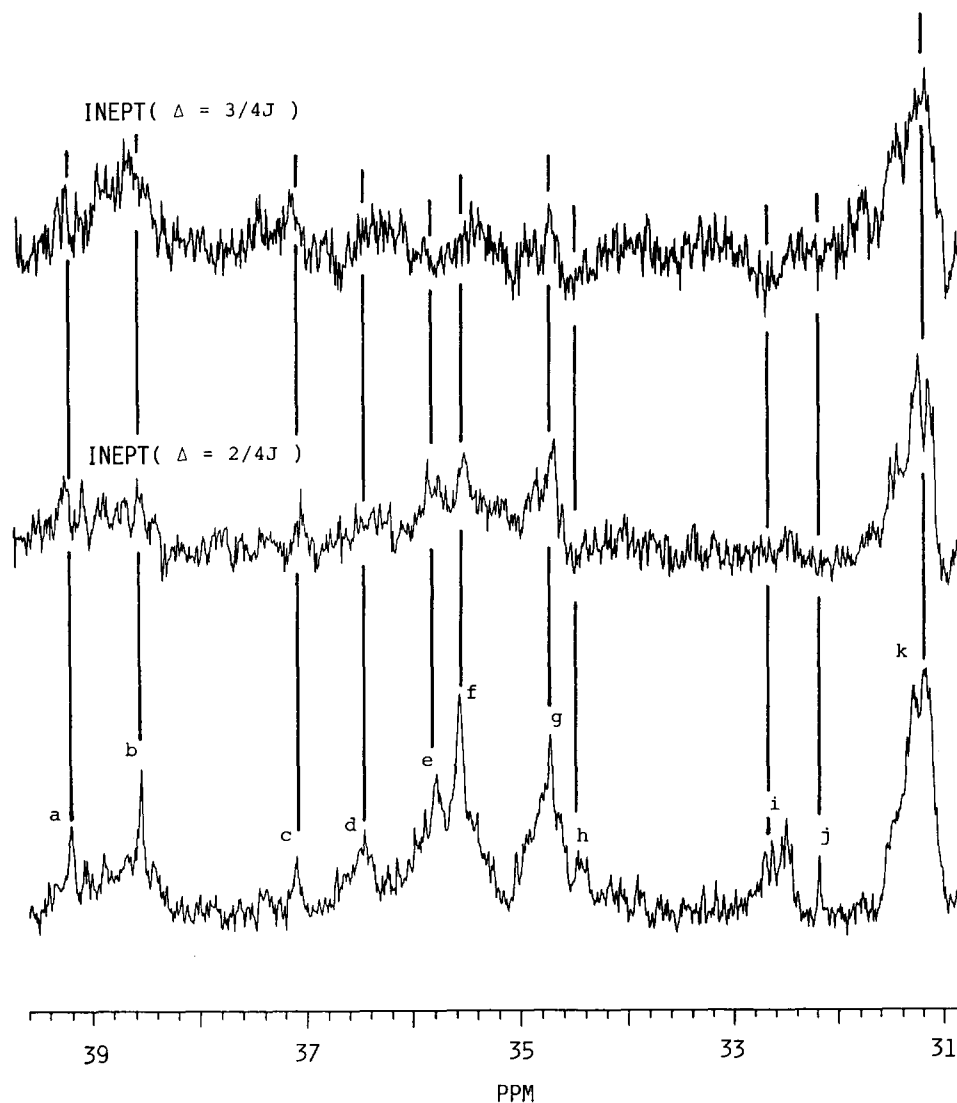
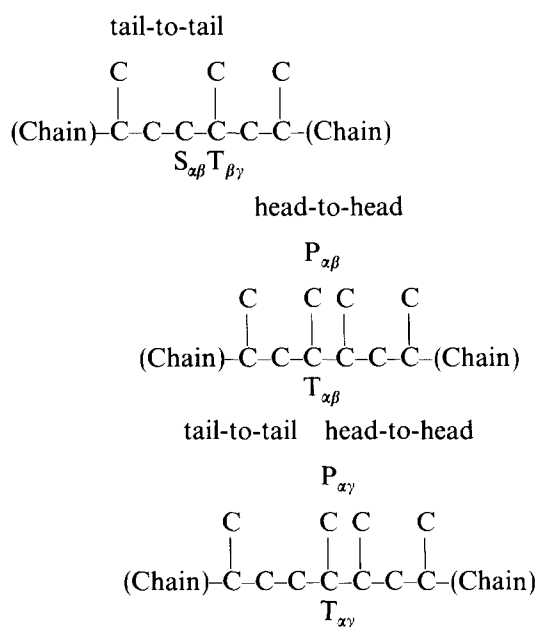


**Figure 8** Regions from 31 to 39 ppm in <sup>13</sup>C n.m.r. (bottom), INEPT ( $\Delta = 2/4J$ , middle), and INEPT ( $\Delta = 3/4J$ , top) spectra of AS6. <sup>1</sup>H-<sup>13</sup>C spin-spin coupling constant,  $J$ , is set to be 125 Hz

are methylene resonances and peak c is a methine resonance. INEPT spectrum obtained with  $\Delta=2/4J$ , where only methine peaks are observed, indicates that peaks a, b, e, f, g and k are composed of methine resonances. Line shapes of peaks a, b, e, f, g, and k in the  $^{13}\text{C}$  normal spectrum are different from those in the INEPT spectrum ( $\Delta=2/4J$ ). In the INEPT spectrum ( $\Delta=3/4J$ ), peaks a, b, e, f, and g are not observed clearly and the profile of the peak k is different from that in the  $^{13}\text{C}$  n.m.r. and INEPT ( $\Delta=2/4J$ ) spectra. These results suggest that overlaps of methylene and methine resonances occur in this spectral region. According to previous assignments<sup>24,25</sup>, peaks h, i and j are assigned to  $S_{\gamma\alpha\beta\gamma}$  and  $S_{\beta\alpha\beta\gamma}$  or  $S_{\beta\alpha\beta\delta}$  carbons, respectively, and peaks a, b, e, f, g and k arise from resonances of  $T_{\alpha\gamma}$  (peaks a and b),  $T_{\alpha\beta}$  (peaks e, f, and g), and  $T_{\beta\gamma}$  (peak k) carbons. The methine peak c has never been identified. Overlapping of methylene and methine resonances is supported by broad chemical shift bands of  $S_{\alpha\beta}$  and  $T_{\alpha\beta}$  carbons calculated via the gamma effect method<sup>25</sup>. In Figure 2 are shown peaks of  $P_{\alpha\beta}$  and  $P_{\alpha\gamma}$  carbons. Thus, present polypropylenes contain the following head-to-head and tail-to-tail arranged propylene units.



The respective intensities of  $P_{\alpha\beta}$  and  $P_{\alpha\gamma}$  carbon peaks are nearly equal to that of carbon 1 in the structure I. Therefore, the contents of head-to-head and tail-to-tail arranged units per chain are  $10^{-3}$  order.

## CONCLUSIONS

Microstructures in polypropylenes (A, B) prepared with  $\text{TiCl}_4/\text{MgCl}_2\text{-Et}_3\text{Al}$  and  $\text{Ti}(\text{O}i\text{Bu})\text{Cl}_3/\text{MgCl}_2\text{-Et}_3\text{Al}$  catalytic systems were determined by  $^{13}\text{C}$  and  $^1\text{H}$  n.m.r. spectroscopy. Pentad tacticities of these samples were reasonably reproduced by the two-site model for the stereospecific polymerization. The optimum values of the model parameters elucidated that the displacement of Cl ligand around the titanium by  $\text{O}i\text{Bu}$  reduces the strength of the steric control at the IPP site. The chain-end structures were investigated by  $^1\text{H}$  and  $^{13}\text{C}$  n.m.r. spectra of boiling hexane soluble fractions (AS6 and BS6) of whole polymers. ( $^{13}\text{C}$  n.m.r. spectra of AS6 and BS6 are practically identical over the whole resonance regions.) The detected structures verified that the chain transfer

of propagating species to the propylene monomer terminates the propagation reaction and regenerates initiating species. The two-site model analysis for the tactic structures at the chain end indicated that the steric controls of the initiation reactions at both sites are as strong as those of the propagation reactions. Further, it was found that these polypropylenes contain the regioirregularity such as head-to-head and tail-to-tail structures whose contents per chain are  $10^{-3}$  order.

## ACKNOWLEDGEMENTS

The authors wish to thank Associate Professor Tetsuo Asakura of Tokyo University of Agriculture and Technology for his helpful advice on the analysis of inverted structures in polypropylenes. T. H. thanks Tokuyama Soda Co., Ltd. for leave from the company to develop this study at Tokyo Institute of Technology.

## REFERENCES

- 1 Delbouille, A. and Speltinckx, P. US Patent 3454547, Solvey & Cie
- 2 Delbouille, A. and Derroite, J. L. US Patent 3658772, Solvey & Cie
- 3 Carrick, W. L., Karapinka, G. L. and Turbett, R. J. US Patent 3324095, Union Carbide Corporation
- 4 Carrick, W. L., Turbett, R. J., Karol, F. J., Karapinka, G. L., Fox, A. S. and Johnson, R. N. *J. Polym. Sci. A-1* 1972, **10**, 2609
- 5 Kashiwa, N., Tokuzumi, T., and Fujimura, H. US Patent 3642746, Mitsui Petrochemical Industries
- 6 Kashiwa, N. US Patent 3647772, Mitsui Petrochemical Industries
- 7 Toyota, A., Kashiwa, N. Japan Patent (open) 50-126590, Mitsui Petrochemical Industries
- 8 Luciani, L., Kashiwa, N., Barbe, C. and Toyota, A. Japan Patent (open) 52-151691, Montedison SPA and Mitsui Petrochemical Industries
- 9 Kashiwa, N. and Yoshitake, J. *Makromol. Chem. Rapid Commun.* 1982, **3**, 211
- 10 Schilling, F. C. and Tonelli, A. E. *Macromolecules* 1980, **13**, 270
- 11 Hayashi, T., Inoue, Y., Chûjô, R. and Asakura, T. *Polymer* 1988, **29**, 139
- 12 Randall, J. C. *J. Polym. Sci. Polym. Phys. Edn.* 1976, **14**, 2083
- 13 Zambelli, A., Locatelli, P., Provasoli, A. and Fero, D. R. *Macromolecules* 1980, **13**, 267
- 14 Chûjô, R. *Kagaku* 1980, **36**, 78
- 15 Zhu, S. N., Yang, X. Z. and Chûjô, R. *Polym. J.* 1983, **15**, 859
- 16 Inoue, Y., Itabashi, Y., Chûjô, R. and Doi, Y. *Polymer* 1984, **25**, 1640
- 17 Furukawa, J. *J. Polym. Sci., Polym. Lett. Edn.* 1965, **3**, 23
- 18 Zambelli, A., Locatelli, P. and Bajo, G. *Macromolecules* 1979, **12**, 154
- 19 Zambelli, A., Locatelli, P. and Rigamonti, E. *Macromolecules* 1979, **12**, 156
- 20 Zambelli, A., Locatelli, P., Sacchi, M. C. and Rigamonti, E. *Macromolecules* 1980, **13**, 798
- 21 Zambelli, A., Sacchi, M. C., Locatelli, P. and Zannoni, E. *Macromolecules* 1982, **15**, 211
- 22 Hayashi, T., Inoue, Y., Chûjô, R. and Asakura, T. *Macromolecules* 1988, **21**, 2765
- 23 Zambelli, A. and Gatti, G. *Macromolecules* 1978, **11**, 485
- 24 Cheng, H. N. *Polymer Bull.* 1985, **14**, 347
- 25 Asakura, T., Nishiyama, Y. and Doi, Y. *Macromolecules* 1987, **20**, 616
- 26 Burum, D. P. and Ernst, R. R. *J. Magn. Reson.* 1980, **39**, 163
- 27 Doddrell, D. M. and Pegg, D. T. *J. Am. Chem. Soc.* 1980, **102**, 6388
- 28 Grubisic, Z., Rempp, P. and Benoit, H. *J. Polym. Sci. (B)* 1967, **5**, 753
- 29 Ogawa, T., Tanaka, S. and Hoshino, S. *Kobunshi Kagaku* 1972, **29**, 6
- 30 Cheng, H. N. and Smith, D. A. *Macromolecules* 1986, **19**, 2065
- 31 Zambelli, A., Locatelli, P., Bajo, G. and Bovey, F. A. *Macromolecules* 1975, **8**, 687



*Microstructure of polypropylenes: T. Hayashi et al.*

- 32 Kawamura, H., Hayashi, T., Inoue, Y. and Chūjō, R. *Macromolecules* in press
- 33 de Hann, J. W., van de Ven, L. J. M., Wilson, A. R. N., van der Hout-Lodder, A. E., Altona, C. and Faber, D. H. *Org. Magn. Reson.* 1976, **8**, 477
- 34 Pouchert, C. J. and Campbell, J. R. 'The Aldrich Library of NMR Spectra', Vol. 1, Aldrich Chemical Company, Inc., Milwaukee, Wisconsin, 1974, p. 23
- 35 Boor, J. Jr. 'Ziegler-Natta Catalysts and Polymerizations', Academic Press, New York (1979)